ARTICLE OPEN

Application of chemometrics for modeling and optimization of ultrasound-assisted dispersive liquid–liquid microextraction for the simultaneous determination of dyes

Siroos Shojaei [1]✉, Saeed Shojaei[2], Arezoo Nouri[1] and Leila Baharinikoo[3]

As the world population continues to grow, so does the pollution of water resources. It is, therefore, important to identify ways of reducing pollution as part of our effort to significantly increase the supply of clean and safer water. In this study, the efficiency of ultrasound-assisted dispersive liquid–liquid microextraction (UA-DLLME) as a fast, economical, and simple method for extraction malachite green (MG) and rhodamine B (RB) dyes from water samples is investigated. In optimal conditions, the linear dynamic range (LDR) for RB and MG is 7.5–1500 ng mL^{-1} and 12–1000 ng mL^{-1}, respectively. The limit of detection (LOD) is 1.45 ng mL^{-1} and 2.73 ng mL^{-1}, and limit of quantification (LOQ) is 4.83 ng mL^{-1} and 9.10 ng mL^{-1} for RB and MG, respectively. Extraction efficiency is obtained in the range of 95.53–99.60%. The relative standard deviations (RSD) in real water and wastewater samples are less than 3.5. The developed method is used successfully in the determination of RB and MG dyes from water samples and there are satisfactory results.

INTRODUCTION

The goals of sustainable development include 17 items, one of which is to study the issue of clean water and sanitation. Globally, dyes are known to be one of the major contributors of water contamination that reduces access to clean potable water[1–5]. There are more than one hundred thousand types of dyes in the world, and 7×10^5 tons of these dyes are produced every year by the textile industry. Studies showed that 15% of the total production of dyes ends up as industrial wastewater during the production process, which is of great concern. Since dyes are highly soluble in water, they are regarded as water pollutants and their occurrence is found at trace levels in industrial wastewater[6–8]. Dyes may dramatically reduce the penetration of light into water, increase suspended particles, and may affect turbidity. Moreover, because of their nature as aromatic and chlorinated in water, they will be hazardous to human and animal health. Dyes have side effects on human health including allergic reactions and asthma, children hyper-activity, DNA damage, and cancer. Many of these dyes are not biodegradable biologically. Nowadays, the removal of dyes from wastewater is of paramount importance because of increased public concern. For this reason, the use of dyes is strictly controlled around the world. As a result, it is indispensable to use reliable and accurate methods to measure the presence of dye in the environment and ensure its removal[9,10]. Malachite green is a dark green solid crystalline substance widely used to dye cotton, acrylic fibers, and also as a strong fungicide to remove foreign parasites in fish farms. The solubility of malachite green in water is 66.67 g L^{-1}. Rhodamine B is a chemical compound which is used as a tracer dye in water. Rhodamine B is highly toxic which is used as a dye in textile and cosmetics industries. Rhodamine B is 400 g L^{-1} soluble in acetic acid solution. Many adverse effects such as carcinogenicity, mutagenicity, severe toxic effects, chromosome failure, and tumorigenesis in fish, humans, and

other mammals have been observed after malachite green and rhodamine B were used[11–14]. Thus, it is important to remove these dyes from the aquatic environment. There are several analysis methods that could be used to determine the dye/s such as capillary electrophoresis, thin layer chromatography, high performance liquid chromatography (HPLC), electrochemistry, voltammetry, and spectrophotometry. Spectrophotometric methods have become one of the most widely used analytical methods in laboratories and various industries due to their ease of use, acceptable limit of detection, and low initial and operational costs[15–23]. Moreover, one of the most significant and common applications in quality control is dye analysis which can determine the dye values in different samples. The step of sample preparation is required before instrumental analysis. One of the extraction methods is liquid–liquid extraction (LLE). Today, the LLE method is less used due to the high consumption of organic solvents, high consumption of dispersant solvent, and also the long time of the experiment[24–27]. To eliminate or reduce the above-mentioned disadvantages, microextraction methods such as dispersive liquid–liquid microextraction (DLLME) technique are used for preconcentration and extraction of very small amounts of different samples[28,29]. This is a simple and fast method which consists of three phases: (1) Extractor phase: it usually has density higher than water, such as ethylene tetrachloride, chloroform, carbon tetrachloride. (2) Disperser solvent: it must have high solubility in both extraction and aqueous phases, such as methanol, ethanol, acetone, and acetonitrile. (3) The water phase: the sample is located in it. When the extracting and dispersing phases are mixed and rapidly injected into the sample solution, the extracting solvent is uniformly and completely dispersed in the aqueous phase by the dispersing solvent, and tiny drops of the extracting solvent cause turbidity in the sample solution. In this case, there is a high contact between the surface of extracting solvent and the

[1]Department of Chemistry, University of Sistan and Baluchestan, Zahedan, Iran. [2]Department of Arid and Mountainous Regions Reclamation, Faculty of Natural Resources, University of Tehran, Tehran, Iran. [3]Department of Analytical Chemistry, Faculty of chemistry, University of Mazandaran, Babolsar, Iran. ✉email: shojaeisiroos@gmail.com

aqueous phase, and because of rapid equilibrium, the extraction time is very short (a few seconds). Then, the extraction solvent containing the analyte can be easily separated by centrifuges. This technique has many advantages such as high sensitivity and selectivity, high extraction efficiency, high speed, and use of small volume of organic solvent. Due to the mentioned advantages, DLLME technique can be widely used in the extraction of analyte from water, food matrix, etc.[30–32]. One of these methods is the use of ultrasonic waves. The mechanism of action of ultrasonic waves is due to the phenomenon of cavitation or the formation of very small bubbles that under the effect of contraction and expansion instantaneously create extreme heat and pressure. This condition causes physicochemical effects on adjacent molecules and increases permeability. For this reason, this process performs the extraction operation in a shorter time and at a lower temperature. Cavitation involves the appearance, growth, and disintegration of bubbles in a liquid. Ultrasound waves increase the mass transfer of materials so that the use of ultrasound can play a significant role in increasing performance, increasing extraction rate, achieving reduced extraction time, and reducing energy consumption[33,34]. The general method to examine factors affecting the process is the method of changing one factor at a time. This method can only examine the effect of each factor separately, but does not explain the fact that different factors can intensify or neutralize each other. Today, statistical and mathematical methods such as response surface methodology (RSM) are used to solve this problem[35]. Such a method uses fewer tests compared to one-factor-at-a-time method, which reduces time, cost, and material savings. Central composite design (CCD) is one of the most important RSM designs that generally requires 5 levels for each factor. When designing is applied, all coefficients of the quadratic regression model and the relationship between various factors are considered. Thus, the optimal values of each variable and the degree of importance of each of them can be easily determined[36,37]. The aim of current work was to investigate the rate of extraction of RB and MG dyes from aqueous solutions. For this purpose, selected effective factors were entered at different levels in the RSM. Experiments were designed by Design Expert software. Then, based on the obtained results, the best formulation with the highest efficiency was used to extract RB and MG dyes from water samples. Due to the applicability of this method, the results can be used to extract these dyes in various industries such as fish ponds and textiles.

RESULTS AND DISCUSSION

Selection of types of extraction and dispersive solvent

When it comes to the liquid–liquid micro-extraction technique, the type of extraction solvent and the type of disperser solvent are influential in the amount of analyte extraction. According to research, the use of solvents such as chloroform and trichloromethane as the extraction solvent and also solvents such as methanol and ethanol as the dispersive solvent were used more. In order to study more, several similar solvents were investigated, the results of which are presented in Figs. 1 and 2. The results show that chloroform was the most efficient extraction solvent (Fig. 1). This is probably due to the high solubility of RB and MG dyes in chloroform, which has high dielectric stability and polarity. The disperser solvent must have a high solubility in both the organic and aqueous phases. Figure 2 shows variation of disperser solvents against recoveries; the results show ethanol as the most efficient dispersive solvent. The highest extraction efficiencies were obtained for chloroform and ethanol compared to other extraction solvents and dispersive solvents. Therefore, chloroform and ethanol were used for UA-DLLME experiments. Then, the effect of the volume of the extraction solvent and the dispersive
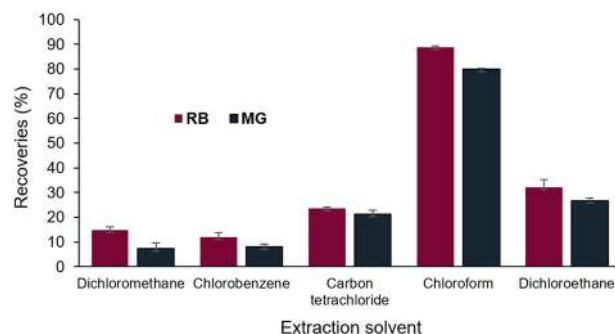
Fig. 1 Influence of type of extraction solvent on extraction efficiency of the dyes. Extraction conditions: water sample volume: 10 mL, spiked concentration: 500 ng mL^{-1}, dispersive solvent: ethanol (760 µL), sonication time: 4 min, pH: 5, centrifuge rate: 3500 rpm. Error bars represent standard deviations.
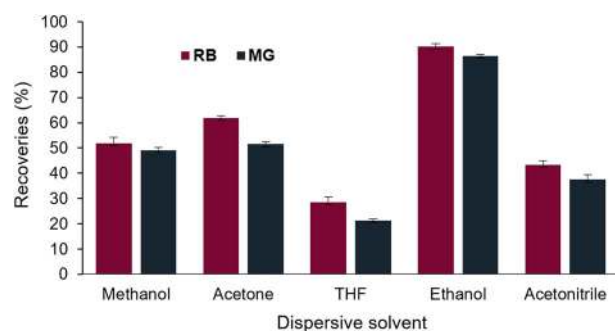
Fig. 2 Influence of type of dispersive solvent on extraction efficiency of the dyes. Extraction conditions: water sample volume: 10 mL, spiked concentration: 500 ng mL^{-1}, extraction solvent: chloroform (120 µL), sonication time: 4 min, pH: 5, centrifuge rate: 3500 rpm. Error bars represent standard deviations.

solvent on the extraction efficiency was investigated and optimized by RSM.

Centrifuge rate selection

Centrifugation is an essential step in DLLME to separate the extractant droplet from the aqueous sample, thereby preconcentrating the analytes. In a DLLME method, the phase separation is achieved by centrifugation. Therefore, the dispersed fine droplets of the extraction phase are sedimented at the bottom of a conical test tube. Then, the sedimented phase is removed using a micro-syringe to be analyzed by UV/Vis spectrophotometer. The effect of centrifuge speed on extraction efficiency at 1000–4500 rpm was investigated. As shown in Fig. 3, the extraction efficiency increases to 3500 rpm and reaches its maximum value and then remains constant. The low extraction efficiency at low speeds is due to the fact that the separation of phases and settling is not complete. Based on the results of this step, the speed of 3500 rpm, which was the highest extraction efficiency for RB and MG, was selected as the optimal values for the next stages of the experiment.

Response surface methodology

In order to establish the relationship between the dependent variables with the independent variables and to fit the model, regression analysis and ANOVA were used. The quadratic polynomial equation was fitted to the dependent variables. Using the statistical method of response level, the following equations were obtained, which show the experimental relationship between the extraction efficiency and the coded test variables.
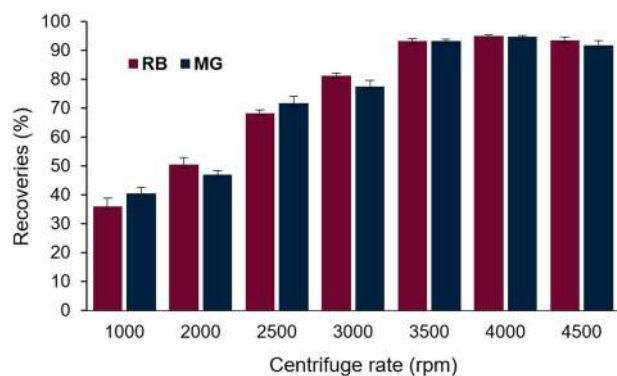
Fig. 3 Effect of centrifuge rate on extraction efficiency. Extraction conditions: water sample volume: 10 mL, spiked concentration: 500 ng mL^{-1}, extraction solvent: chloroform (120 µL), dispersive solvent: ethanol (760 µL), sonication time: 4 min, pH: 5. Error bars represent standard deviations.

These models were introduced after deleting variables that were not statistically significant.

$$Y_{RB} = +90.85 + 7.95^* A + 8.04^* B + 10.54^* C + 4.94^* D - 7.36^* E$$
$$+ 0.96^* AB + 1.07^* AC + 1.64^* AD - 1.32^* AE + 0.36^* BC$$
$$+ 1.80^* BD - 0.71^* BE + 2.25^* CD - 0.40^* CE - 1.69^* DE$$
$$- 6.52^* A^2 - 4.65^* B^2 - 8.93^* C^2 - 3.24^* D^2 - 2.37^* E^2$$

$$(1)$$

$$Y_{MG} = +91.53 + 6.15^* A + 8.48^* B + 7.84^* C + 7.53^* D - 9.12^* E$$
$$+ 0.27^* AB - 0.20^* AC + 0.55^* AD + 0.48^* AE - 0.64^* BC$$
$$- 0.82^* BD + 1.18^* BE + 0.12^* CD + 0.74^* CE + 0.86^* DE$$
$$- 4.37^* A^2 - 2.74^* B^2 - 5.58^* C^2 - 2.27^* D^2 - 3.14^* E^2$$

$$(2)$$

The results and analysis of variance are shown in Supplementary Table 1 and Supplementary Table 2, respectively. This study showed that the second-order model is suitable for predicting the results of the RB and MG extraction process. The coefficient R^2 represents the ratio of the total changes in the response predicted by the model and indicates the ratio of the sum of squares due to regression (SSR) to the total sum of squares (SST). The proximity of R^2 to 1 is desirable and a favorable agreement with Adj-R^2 is necessary. The magnitude of R^2 confirms the satisfactory conformity of the experimental data to the second-order model. Considering that in this study, in all cases, the coefficient R^2 and the coefficient Adj-R^2 were higher than 0.99. Therefore, the second-order model had a good fit on the data. The test fit of lack test describes data changes around the fitted model. If the model does not fit well, this test is significant. The fitting weakness test for the second-order model fitted was not significant for the responses obtained in this study (0.2919 for RB and 0.7371 for MG), which confirms that good fit of the data is selected on the model. In Fig. 4a, b, the graph of the values predicted by the quadratic model versus the experimental values obtained from the measured response can be seen. This graph showed $R^2 > 99.8\%$ for both dyes (Supplementary Table 1) and it represents that the prediction capacity of the proposed quadratic model is high. The residual distribution diagram did not show a specific trend indicating the increase or decrease of variance in relation to the fitted values obtained from the application of this method, which is used to check the assumption that the residual variance is constant. Therefore, the assumption that the variance is constant was accepted (Fig. 4c, d). No sinusoidal changes were observed in the residual distribution diagram in relation to the order in which

the residues were randomly distributed around zero and used to examine the independence of the data. Therefore, the assumption of data independence was accepted and the selected model is suitable for data analysis (Fig. 4e, f).

In Figs. 5 and 6, the three-dimensional surfaces of the answers can be visualized. They were obtained with the proposed quadratic degree model. In Figs. 5 and 6, the interaction of variables on the extraction rate was investigated. The pH of the solution affects the chemistry of the aqueous medium and therefore the pH is an important parameter during the extraction process. The effect of pH on extraction in the pH range (3–7) was investigated. The extraction rate increased with increasing the pH from 3 to 5, with a maximum efficiency for pH of 5 for both dyes. At low pH, due to the positive charge, there is more dissolution in water, which prevents the extraction of dyes, while at low pH, the predominant form is the anionic form and its extraction is limited to chloroform. Therefore, the optimum pH was considered 5. Ultrasonication time (1–5 min) was another parameter studied in this research. Extraction time is the interval between the injection of the extraction mixture into the sample solution and the centrifuge. The results showed that in a very short time after cloud formation, the extraction reached equilibrium. Due to the fact that after 4 min, no significant increase in extraction efficiency was observed, so the equilibrium time of 4 min was selected. This fast time is the advantage of the present method which prevents the transfer of hydrophilic compound to the extraction phase. To investigate the effect of the volume of the extraction solvent on the extraction efficiency, different volumes of chloroform (50–250 µL) were added to the solution. Based on the results, the extraction efficiency of the analyte in the chloroform volume is maximum at 120 µL and then with increasing volume, the extraction efficiency decreased due to the decrease of the concentration factor and because of the increase of the volume of the precipitated phase. Therefore, in order to obtain a high concentration factor and efficiency for the extraction of RB and MG, 120 µL of chloroform was selected as the optimal volume. In the study of the effect of the volume of disperser solvent (200–1000 µL), based on the obtained results, with increasing the volume of ethanol to 760 µL, an increase in extraction efficiency was observed and then there was a decrease. Because when using small amounts of ethanol, the cloud phase is not completely formed, as a result, %R (recovery) decreases. On the other hand, when the volume of ethanol increased to 1000 µl, the %R (recovery) dropped due to the decrease in the species distribution constant. Therefore, a volume of 760 µL of ethanol was selected as the optimal volume. Salt can increase the extraction efficiency of many extraction methods because by increasing the ionic strength of the solution sample, the aqueous phase distribution coefficient can be increased. This phenomenon helps to increase the combination of the acceptor phase for analyte molecules. In this study, sodium chloride was added to the analytical samples. The results showed that with increasing the percentage of salt, the percentage of extraction decreased. The addition of salt increases the volume of the sedimentation phase and reduces the diffusion phenomenon, as a result of which the extraction efficiency decreases. So, the experiments were carried out without ionic strength (salt).

Optimization of CCD

Mathematical Optimization, also called Mathematical Programming, is the process by which the best answer (according to a set of criteria) is selected from a set of possible answers to a particular problem. If designers can save time and money with optimization methods, they will be able to create better methods. Basically, in chemistry and environment, optimization is to maximize the determination of pollutants and achieve standard values of response (%R), which also leads to
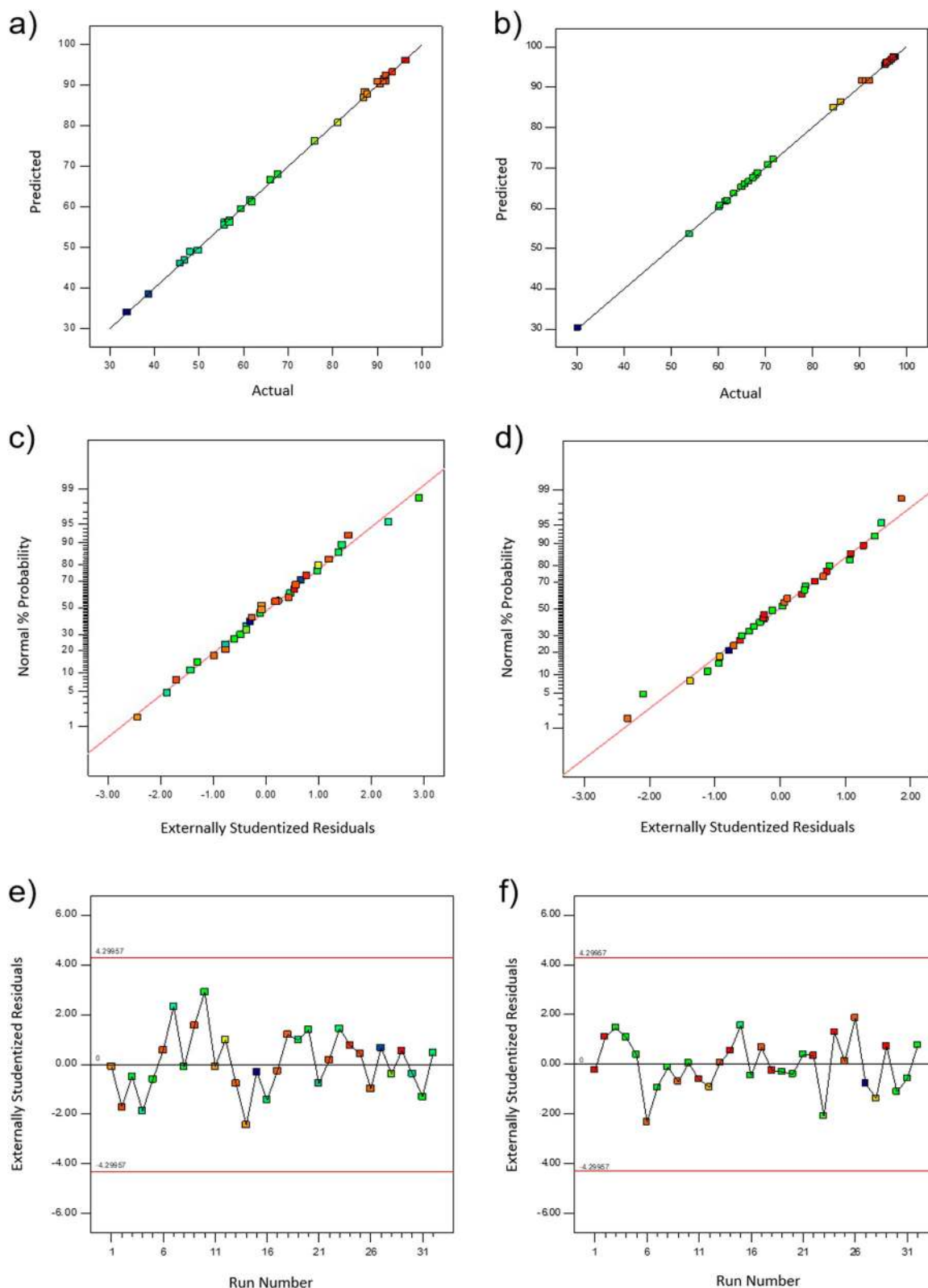
Fig. 4 **Residuals of plots. a, b** The experimental data versus predicted data for extraction of RB and MG, **c, d** normal plot of residuals forextraction of RB and MG, **e, f** residuals versus runs for extraction of RB and MG (Model Statistics: Quadratic, Degrees of freedom: 20, Sum of squares (RB): 11707.52, Sum of squares (MG): 9205.77, Adj- R2 (RB): 99.73%, Adj- R2 (MG): 99.74%, Adeq-Precision (RB): 94.160, Adeq-Precision (MG):194.167).

sustainable development of 12 SDG (creating sustainable production and consumption patterns). In order to achieve maximum efficiency, optimization was performed using Design Expert software. The optimal mean %R obtained for the variables (pH of solution, ultrasonication time, extraction volume, and disperser volume) was 97.68% and 98.51% for RB and MG, respectively, with a predicted value of 99.07% and 99.74%, with a relative usefulness of 1.00 which shows that the
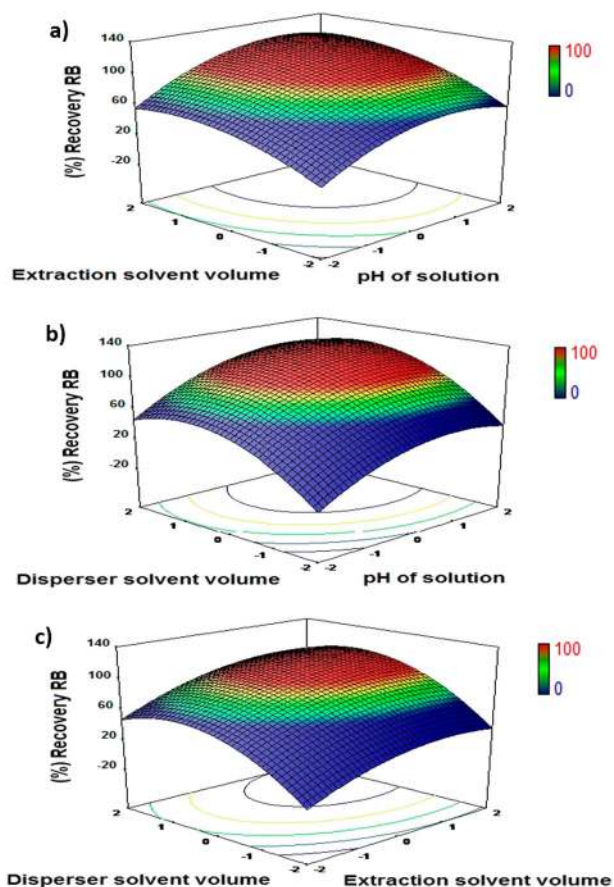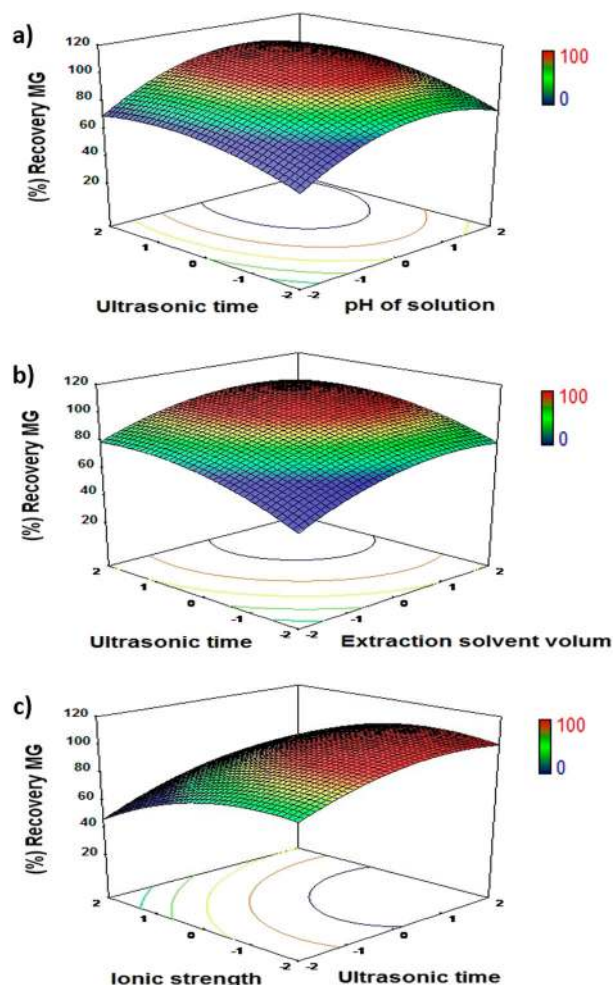
Fig. 5 The response surface plots showing the effects of variables on extraction of RB. a The interaction of extraction solvent volume and pH of solution, b the interaction of disperser solvent volume and pH of solution, c the interaction of disperser solvent volume and extraction solvent volume (experimental conditions: ionic strength: 0.0–10.0 w/v%, extraction solvent: chloroform (50–250 µL), sonication time: 1–5 min, dispersive solvent: ethanol (200–1000 µL), pH: 3–7, water sample volume: 10 mL, centrifuge rate: 3500 rpm, spiked concentration: 500 ng mL^{-1}).

Fig. 6 The response surface plots showing the effects of variables on extraction of MG. a The interaction of ultrasonication time and pH of solution, b the interaction of ultrasonication time and extraction solvent volume, c the interaction of ionic strength and ultrasonication time (experimental conditions: ionic strength: 0.0–10.0 w/v%, extraction solvent: chloroform (50–250 µL), sonication time: 1–5 min, dispersive solvent: ethanol (200–1000 µL), pH: 3–7, water sample volume: 10 mL, centrifuge rate: 3500 rpm, spiked concentration: 500 ng mL^{-1}).

model is highly desirable. The model predicted to achieve maximum extraction of both dyes at pH 5 was 120 µL of extraction solvent, 760 µL of disperser solvent, 4 min of ultrasound, and no salt.

Method validation
Table 1 shows some analytical parameters of the method such as preconcentration factor (PF), enrichment factor (EF), extraction recovery (%ER), limit of detection (LOD), relative standard deviation (%RSD), the correlation coefficient of the calibration diagram, linear range. In order to draw the calibration curve and determine the linear range of the method, standard aqueous solutions of RB and MG dyes were prepared at a concentration of 100 µg mL^{-1} and then the different dilutions of the dye solutions were applied. The relative standard deviation of the method was obtained by conducting 5 repetitive experiments using the standard solution of RB and MG dyes at a concentration of 500 ng mL^{-1} under optimal conditions. Linearity was observed over the range of 7.5–1500 ng mL^{-1} and 12–1000 ng mL^{-1} for RB and MG, respectively. The enrichment factor was calculated by dividing the slope of the precondensation calibration curve to the slope of the calibration curve without precondensation (direct).

Real sample analysis
The application of the developed method for extraction and determination of RB and MG in water samples (deionized water, tap water, water of Sistan lake, and wastewater) was tested. Each sample was examined by spiking the RB and MG dyes separately in the proposed method under optimal conditions. The results are shown in Table 2. The recovery percentage of the method was calculated using water samples to which 500 ng mL^{-1} of RB and MG were added manually. Analyte extraction recovery was between 95.53 and 99.60%. As shown, the proposed method can be reliably used to determine the objectivity of RB and MG in environmental water samples.

Comparison with other methods
The analytical performance of the proposed method is compared with various published methods to determine RB and MG. As shown in Table 3, the proposed method has detection limits and linear range amplitudes comparable or better than previously reported methods[38,39,42]. The current extraction method is a simple, inexpensive, and available method compared to HPLC and

Table 1. Analytical characteristics of the developed method.

Analyte	Limit of detection[a]	Limit of quantification[a]	Linear dynamic range[a]	Correlation coefficients	Regression equation	Preconcentration factor	Enrichment factor
RB	1.45	4.83	7.5–1500	0.9979	$y = 0.0008x + 0.0013$	83.33	86.63
MG	2.73	9.10	12–1000	0.9983	$y = 0.0011x - 0.0043$	83.33	97.54

[a]All concentrations are based on $ng\,mL^{-1}$.

Table 2. Spiked recoveries (%) of real water samples.

Samples	Added ($ng\,mL^{-1}$)		Found ($ng\,mL^{-1}$)		Recoveries% ± RSD (%)	
	RB	MG	RB	MG	RB	MG
Deionized water	500	500	488.40	492.55	97.68 ± 1.6	98.51 ± 3.4
Tap water	500	500	498.03	496.59	99.60 ± 0.9	99.31 ± 2.7
Water of Sistan lake	500	500	477.65	495.77	95.53 ± 3.2	99.15 ± 2.6
Wastewater	500	500	491.03	489.95	98.20 ± 3.8	97.99 ± 1.9

Extraction conditions: water sample volume: 10 mL, dispersive solvent: ethanol (760 µL), extraction solvent: chloroform (120 µL), sonication time: 4 min, pH: 5, centrifuge rate: 3500 rpm.

Table 3. Comparison of different methods for extraction of RB and MG dyes with developed methods.

Technique	Detection	Analyte	LDR[a]	LOD[b]	LOQ[c]	PF[d]	Ref.
MSA-DLLME[e]	HPLC–UV/Vis	RB	5–1000 ($ng\,mL^{-1}$)	1.15 ($ng\,mL^{-1}$)	3.82 ($ng\,mL^{-1}$)	48	[38]
CPE[f]	Spectrophtometric	MG	4–500 ($ng\,mL^{-1}$)	1.20 ($ng\,mL^{-1}$)			[39]
DES-DLLME[g]	HPLC–UV/Vis	MG	0.2–500 ($µg\,L^{-1}$)	0.03 ($µg\,L^{-1}$)	0.09 ($µg\,L^{-1}$)	95	[40]
MSPE[h]	HPLC–UV/Vis	RB	0.50–150 ($µg\,L^{-1}$)	0.08 ($µg\,L^{-1}$)		25	[41]
DLLME[i]	Spectrophtometric	RB	0.1–3 ($µg\,L^{-1}$)	2.1 ($µg\,L^{-1}$)		330	[42]
EME[j]	Ion mobility spectrometry	MG	5–250 ($ng\,mL^{-1}$)	1.50 ($ng\,mL^{-1}$)		150	[43]
MSPE[k]	Spectrofluorimetry	RB	0.35–5 ($µg\,L^{-1}$)	0.1 ($µg\,L^{-1}$)	0.35 ($µg\,L^{-1}$)		[44]
UA-DLLME[l]	Spectrophtometric	MG	12–1000 ($ng\,mL^{-1}$)	2.73 ($ng\,mL^{-1}$)	9.10 ($ng\,mL^{-1}$)	83.33	This work
		RB	7.5–1500 ($ng\,mL^{-1}$)	1.45 ($ng\,mL^{-1}$)	4.83 ($ng\,mL^{-1}$)		

[a]Linear dynamic range, [b]Limit of detection, [c]Limit of quantification, [d]Preconcentration Factor, [e]Magnetic stirring assisted dispersive liquid–liquid microextraction, [f]Cloud point extraction, [g]Deep eutectic solvent-dispersive liquid–liquid micro-extraction, [h]Magnetic solid phase extraction, [i]Dispersive liquid–liquid microextraction, [j]Electromembrane extraction, [k]Micro solid phase extraction, [l]Ultrasound-assisted-dispersive liquid–liquid microextraction.

GC methods. Extraction time in this work is dramatically short. These results indicate that UA-DLLME is a reproducible and simple method that can be successfully used for preconcentration and extraction of RB and MG dyes in water samples.

In this study, a new method was introduced based on ultrasound-assisted dispersive liquid–liquid microextraction (UA-DLLME) technique in combination with UV/Visible spectrophotometer to measure very small amounts of RB and MG. Then CCD based on response surface methodology was used as an efficient statistical method to reduce the number of experiments and achieve suitable conditions for extraction based on independent variables such as extraction volume, ultrasonication time, disperser volume, ionic strength, and pH of the solution. Optimal conditions for maximum dye extraction were obtained at 4 min sonication time, pH 5, 120 µL of extraction solvent (chloroform), 760 µL of disperser solvent (ethanol), respectively, without adding salt. The maximum experimental extraction for RB and MG was 97.68% and 98.51%, respectively. Also, the results of analysis of real samples and comparison with other measurement methods

(Table 3) showed that this technique can be used as a suitable, fast and sensitive method to determine the dyes of RB and MG in different water samples in other parts of the world. The proposed method offers advantages such as simplicity, low cost, good accuracy, high speed, high enrichment factor, wide linear range, and low detection limit in extraction and measurement due to ultrasonication-enhanced coupling, which could be useful in achieving bio-strategies in relation to SDGs.

METHODS

Reagents and apparatus

All chemicals used in the present work were of analytical grade purity. Carbon tetrachloride, dichloromethane, dichloroethane, chlorobenzene, ethanol, acetone, methanol, acetonitrile, sodium chloride, tetrahydrofuran (THF), hydrochloric acid, and sodium hydroxide were purchased from Merck company (Merck Millipore, Darmstadt, Germany). Standard solutions (100 $µg\,mL^{-1}$) RB and MG dyes were prepared by weighing an appropriate amount of standard dyes and increasing the volume of the solution (100 mL) with distilled water. Working solutions were prepared by suitable

dilution of the standard solution with distilled water. The pH of the solutions was adjusted using the solution of sodium hydroxide and 0.1 M hydrochloric acid. The chemical structure of the dyes is shown in Supplementary Fig. 1. Spectrophotometric measurements were done on a UV/Visible spectrophotometer (2120 UV plus, Optizen) equipped with a 500 μL quartz cell (Outside dim (mm): $45 \times 12.5 \times 12.5$, volume (ml): 0.5, Pathlength: 10 mm and kind: glass) at a maximum wavelength of RB (554 nm) and MG (620 nm). An Ultrasonic device (Skymen, Model: JP-020S, China) was used to create more interaction between extraction solvent and aqueous donor phase. All computations were carried out on a computer with 8 GB DDR4 memory and an Intel Core i3-8130U 2.20 GHZ. Design Expert 10 software was used to investigate the impact of effective parameters on the process.

UA-DLLME procedure

This research examined how the UA-DLLME method was used to reduce environmental impacts and improve clean water to help achieve SDGs. In order to do so, 10 mL of 500 ng mL^{-1} solution containing RB and MG with 120 μL chloroform (extraction solvent) and 760 μL ethanol (disperser solvent) at pH 5 was injected through a syringe into a conical bottom glass tube, and then the mixture was immediately placed in the ultrasound system for 4 min. In this step, RB and MG were extracted by chloroform droplets appearing in the cloud. After 4 min of sonication and centrifugation of the mixture for 3 min at 3500 rpm, phase separation was carried out. After centrifugation, 50 μL of the separated phase was transferred to quartz microcells by a Hamilton syringe for analysis of the dyes using UV/Vis spectrophotometer. Then, the extraction recovery (%R) as a percentage of moles of dyes extracted was calculated on the extraction phase present in the sample solution. After that, the preconcentration factor (PF) was calculated as the ratio of the final dye concentration after the extraction step to the initial dye concentration in the sample solution and the enhancement factor (EF) as the ratio of the slope of the calibration curve after extraction to the slope of the calibration curve before extraction.

RSM based on CCD

Test designs of an experiment are commonly used to evaluate and optimize the efficiency of factors in a process or method to improve performance and minimize test error. RSM based on CCD is one of the experimental designs. This design is a mathematical method that is used to identify important variables and optimal conditions. In fact, this scheme provides accurate models for the method by considering the interaction of parameters. In the present project, a five-factor, five-level CCD based on 32 experimental runs is used. Factors studied included ultrasonication time, solution pH, volume of extracting solvent, volume of dispersant solvent, and salt concentration. The variables were coded independently at five levels: low (-1), high ($+1$), central (0), and axial points as -2 and $+2$, with the ranges and levels of each scale shown in Supplementary Table 1. The complete CCD design matrix is presented in terms of the real independent factor after conducting 32 experiments and calculating the extraction percentage. The correlation between the response and the independent used factors was calculated by the second-order polynomial equation. The parameters and equation of the second-order polynomial model are expressed as follows.

$$(x + a)^n = \sum_{k=0}^{n} \binom{n}{k} x^k a^{n-k} \tag{3}$$

$$y = \beta_0 + \sum_{i}^{k} \beta_i X_i + \sum_{i}^{k} \beta_{ii} X_i^2 + \sum_{i<j}^{k} \sum_{j}^{k} \beta_{ij} X_i X_j + \varepsilon \tag{4}$$

Which is actually the percentage of extraction. X_i and X_j are the variables under consideration. β_0 is the intercept coefficient. β_i, β_{ii}, and β_{ij} are the coefficients of quadratic linear terms. k is the number of independent variables. ε is the error rate. ANOVA statistical model test was to evaluate the quality of experimental data fit and also to evaluate the importance of each variable in the equation by regression model.

DATA AVAILABILITY

The authors declare that [the/all other] data supporting the findings of this study are available within the paper [and its supplementary information files].

REFERENCES

1. Chimhowu, A. O., Hulme, D. & Munro, L. T. The 'New'national development planning and global development goals: processes and partnerships. *World Dev.* **120**, 76–89 (2019).
2. Giannetti, B. F., Agostinho, F., Eras, J. C., Yang, Z. & Almeida, C. M. V. B. Cleaner production for achieving the sustainable development goals. *J. Cleaner Prod.* **271**, 122127 (2020).
3. Qi, M. et al. Pollution reduction and operating cost analysis of municipal wastewater treatment in China and implication for future wastewater management. *J. Clean. Prod.* **253**, 120003 (2020).
4. Shojaei, S., Kalantari, Z. & Rodrigo-Comino, J. Prediction of factors affecting activation of soil erosion by mathematical modeling at pedon scale under laboratory conditions. *Sci. Rep.* **10**, 1–12 (2020).
5. Tortajada, C. Contributions of recycled wastewater to clean water and sanitation sustainable development goals. *npj Clean Water* **3**, 1–6 (2020).
6. dos Santos Silva, P. M. et al. Natural dye from Croton urucurana Baill. bark: extraction, physicochemical characterization, textile dyeing and color fastness properties. *Dyes Pigment.* **173**, 107953 (2020).
7. Du, H. et al. Red dye extracted sappan wood waste derived activated carbons characterization and dye adsorption properties. *Diam. Relat. Mater.* **102**, 107646 (2020).
8. Cinperi, N. C., Ozturk, E., Yigit, N. O. & Kitis, M. Treatment of woolen textile wastewater using membrane bioreactor, nanofiltration and reverse osmosis for reuse in production processes. *J. Clean. Prod.* **223**, 837–848 (2019).
9. Sharma, G. & Kandasubramanian, B. Molecularly imprinted polymers for selective recognition and extraction of heavy metal ions and toxic dyes. *J. Chem. Eng. Data.* **65**, 396–418 (2020).
10. Valley, B., Jing, B., Ferreira, M. & Zhu, Y. Rapid and efficient coacervate extraction of cationic industrial dyes from wastewater. *ACS Appl. Mater. Interfaces* **11**, 7472–7478 (2019).
11. Hamouda, R. A., El-Naggar, N. E. A., Doleib, N. M. & Saddiq, A. A. Bioprocessing strategies for cost-effective simultaneous removal of chromium and malachite green by marine alga *Enteromorpha intestinalis*. *Sci. Rep.* **10**, 1–19 (2020).
12. Muraro, P. C. L. et al. Iron oxide nanocatalyst with titanium and silver nanoparticles: synthesis, characterization and photocatalytic activity on the degradation of Rhodamine B dye. *Sci. Rep.* **10**, 1–9 (2020).
13. Tang, S. H. & Zaini, M. A. A. Development of activated carbon pellets using a facile low-cost binder for effective malachite green dye removal. *J. Clean. Prod.* **253**, 119970 (2020).
14. Yu, C. et al. Multi-channel microfluidic chip coupling with mass spectrometry for simultaneous electro-sprays and extraction. *Sci. Rep.* **7**, 1–9 (2017).
15. Arabi, M. et al. Hydrophilic molecularly imprinted nanospheres for the extraction of rhodamine B followed by HPLC analysis: a green approach and hazardous waste elimination. *Talanta* **215**, 120933 (2020).
16. Hałka-Grysińska, A., Cyrta, A. & Dzido, T. H. Reversed-phase stepwise gradient thin-layer chromatography of test dye mixtures with controlled developing solvent velocity. *J. Chromatogr. A.* **1610**, 460516 (2020).
17. Akpomie, K. G. & Conradie, J. Biogenic and chemically synthesized *Solanum tuberosum* peel–silver nanoparticle hybrid for the ultrasonic aided adsorption of bromophenol blue dye. *Sci. Rep.* **10**, 1–18 (2020).
18. Al-Ghouti, M. A. & Al-Absi, R. S. Mechanistic understanding of the adsorption and thermodynamic aspects of cationic methylene blue dye onto cellulosic olive stones biomass from wastewater. *Sci. Rep.* **10**, 1–18 (2020).
19. Yang, J. et al. Synthesis, spectroscopic characterization, one and two-photon absorption properties and electrochemistry of π-expanded BODIPYs dyes. *Dyes Pigment.* **175**, 108173 (2020).
20. Aralekallu, S., Mohammed, I., Manjunatha, N., Palanna, M. & Sannegowda, L. K. Synthesis of novel azo group substituted polymeric phthalocyanine for amperometric sensing of nitrite. *Sens. Actuators, B.* **282**, 417–425 (2019).
21. Mathiyalagan, S., Mandal, B. K. & Ling, Y. C. Determination of synthetic and natural colorants in selected green colored foodstuffs through reverse phase-high performance liquid chromatography. *Food Chem.* **278**, 381–387 (2019).
22. Mirzajani, R. & Karimi, S. Ultrasonic assisted synthesis of magnetic Ni-Ag bimetallic nanoparticles supported on reduced graphene oxide for sonochemical simultaneous removal of sunset yellow and tartrazine dyes by response surface optimization: application of derivative spectrophotometry. *Ultrason. Sonochem.* **50**, 239–250 (2019).
23. Huang, Y. & Wang, R. An efficient lithium ion imprinted adsorbent using multi-wall carbon nanotubes as support to recover lithium from water. *J. Clean. Prod.* **205**, 201–209 (2018).

24. Suzuki, D., Sato, Y., Kamasaka, H., Kuriki, T. & Tamura, H. Oiling-out effect improves the efficiency of extracting aroma compounds from edible oil. *npj Sci. Food* **4**, 1–11 (2020).

25. Jiang, H. L., Li, N., Cui, L., Wang, X. & Zhao, R. S. Recent application of magnetic solid phase extraction for food safety analysis. *Trends Anal. Chem.* **120**, 115632 (2019).

26. Sprakel, L. M. J. & Schuur, B. Solvent developments for liquid–liquid extraction of carboxylic acids in perspective. *Sep. Purif. Technol.* **211**, 935–957 (2019).

27. Xie, Y. et al. Exploring bubble oscillation and mass transfer enhancement in acoustic-assisted liquid–liquid extraction with a microfluidic device. *Sci. Rep.* **5**, 12572 (2015).

28. Sorouraddin, S. M., Farajzadeh, M. A. & Dastoori, H. Development of a dispersive liquid–liquid microextraction method based on a ternary deep eutectic solvent as chelating agent and extraction solvent for preconcentration of heavy metals from milk samples. *Talanta* **208**, 120485 (2020).

29. Abdallah, O. I. & Ahmed, N. S. Development of a vortex-assisted dispersive liquid-liquid microextraction (VA-DLLME) and LC-MS/MS procedure for simultaneous determination of fipronil and its metabolite fipronil sulfone in tomato fruits. *Food Anal. Methods* **12**, 2314–2325 (2019).

30. Cui, Y. et al. Dispersive liquid–liquid microextraction with high-performance liquid chromatography for the analysis of 1, 4-benzodioxane-6-aldehyde in eliglustat tartrate active pharmaceutical ingredient. *J. Pharm. Biomed. Anal.* **179**, 112988 (2020).

31. Farajzadeh, M. A., Mohebbi, A., Pazhohan, A., Nemati, M. & Mogaddam, M. R. A. Air–assisted liquid–liquid microextraction; principles and applications with analytical instruments. *Trends Anal. Chem.* **122**, 115734 (2020).

32. Kokosa, J. M. Dispersive liquid–liquid microextraction. *Liq. Phase Extr.* **chapter 16**, 473–497 (2020).

33. Sricharoen, P. et al. Sono-synthesized Fe_3O_4–GO–NH_2 nanocomposite for highly efficient ultrasound-assisted magnetic dispersive solid-phase microextraction of hazardous dye Congo red from water samples. *J. Korean Ceram. Soc.* **58**, 1–11 (2020).

34. Sricharoen, P., Limchoowong, N., Techawongstien, S. & Chanthai, S. Ultrasound-assisted emulsification microextraction coupled with salt-induced demulsification based on solidified floating organic drop prior to HPLC determination of Sudan dyes in chili products. *Arab. J. Chem.* **12**, 5223–5233 (2019).

35. Abbasi, S., Mirghorayshi, M., Zinadini, S. & Zinatizadeh, A. A. A novel single continuous electrocoagulation process for treatment of licorice processing wastewater: optimization of operating factors using RSM. *Process Saf. Environ. Prot.* **134**, 323–332 (2020).

36. Abdullah, N., Saidur, R., Zainoodin, A. M. & Aslfattahi, N. Optimization of electrocatalyst performance of platinum–ruthenium induced with MXene by response surface methodology for clean energy application. *J. Clean. Prod.* **277**, 123395 (2020).

37. Bheemanapally, K., Ibrahim, M. M. & Briski, K. P. Optimization of ultra-high-performance liquid chromatography-electrospray ionization-mass spectrometry detection of glutamine-FMOC ad-hoc derivative by central composite design. *Sci. Rep.* **10**, 1–9 (2020).

38. Ranjbari, E. & Hadjmohammadi, M. R. Optimization of magnetic stirring assisted dispersive liquid–liquid microextraction of rhodamine B and rhodamine 6G by response surface methodology: application in water samples, soft drink, and cosmetic products. *Talanta* **139**, 216–225 (2015).

39. Pourreza, N. & Elhami, S. Spectrophotometric determination of malachite green in fish farming water samples after cloud point extraction using nonionic surfactant Triton X-100. *Anal. Chim. Acta* **596**, 62–65 (2007).

40. Farajzadeh, M. A., Mogaddam, M. R. A. & Aghanassab, M. Deep eutectic solvent-based dispersive liquid–liquid microextraction. *Anal. Methods* **8**, 2576–2583 (2016).

41. Chen, J. & Zhu, X. Magnetic solid phase extraction using ionic liquid-coated core–shell magnetic nanoparticles followed by high-performance liquid chromatography for determination of Rhodamine B in food samples. *Food Chem.* **200**, 10–15 (2016).

42. Unsal, Y. E., Soylak, M. & Tuzen, M. Dispersive liquid–liquid microextraction–spectrophotometry combination for determination of rhodamine B in food, water, and environmental samples. *Desalin. Water Treat.* **55**, 2103–2108 (2015).

43. Mirzaei, F., Nilash, M. M. & Fakhari, A. R. Development of a new electromembrane extraction combined with ion mobility spectrometry for the quantification of malachite green in water samples. *Int. J. Ion Mobil. Spectrom.* **23**, 1–8 (2020).

44. Bagheri, H., Daliri, R. & Roostaie, A. A novel magnetic poly (aniline-naphthylamine)-based nanocomposite for micro solid phase extraction of rhodamine B. *Anal. Chim. Acta* **794**, 38–46 (2013).

ACKNOWLEDGEMENTS

AUTHOR CONTRIBUTIONS

Authors read and approved the final manuscript.

COMPETING INTERESTS

The authors declare no competing interests.

ADDITIONAL INFORMATION

Supplementary information The online version contains supplementary material available at https://doi.org/10.1038/s41545-021-00113-6.

Correspondence and requests for materials should be addressed to S.S.

Reprints and permission information is available at http://www.nature.com/reprints

Publisher's note Springer Nature remains neutral with regard to jurisdictional claims in published maps and institutional affiliations.